isvr Institute of Sound and Vibration Research

Simulation of Multichannel Free Field Control Experiment

C. Bordier

ISVR Technical Memorandum No 898

December 2002

University of Southampton

SCIENTIFIC PUBLICATIONS BY THE ISVR

Technical Reports are published to promote timely dissemination of research results by ISVR personnel. This medium permits more detailed presentation than is usually acceptable for scientific journals. Responsibility for both the content and any opinions expressed rests entirely with the author(s).

Technical Memoranda are produced to enable the early or preliminary release of information by ISVR personnel where such release is deemed to the appropriate. Information contained in these memoranda may be incomplete, or form part of a continuing programme; this should be borne in mind when using or quoting from these documents.

Contract Reports are produced to record the results of scientific work carried out for sponsors, under contract. The ISVR treats these reports as confidential to sponsors and does not make them available for general circulation. Individual sponsors may, however, authorize subsequent release of the material.

UNIVERSITY OF SOUTHAMPTON

INSTITUTE OF SOUND AND VIBRATION RESEARCH

SIGNAL PROCESSING & CONTROL GROUP

SIMULATION OF MULTICHANNEL FREE FIELD CONTROL EXPERIMENT

by

Claire Bordier

ISVR Technical Memorandum No. 898

December 2002

Authorised for issue by
Prof S J Elliott
Group Chairman

ACKNOWLEDGEMENTS :

I would like to thank my supervisor, Professor Stephen Elliot, for his guidance and help throughout my stay at the ISVR.
Thanks are also due to Paolo Gardonio, responsible for the European Doctorate in Sound and Vibration Studies, the programme that allowed me to come at the ISVR.
Thanks also to Joyce Shotter for her help in every administrative step.
Finally, I would like to thank all members of the Signal Processing and Control Group for their help and their welcome.

Contents

Several experiments have been driven in the anechoic theatre of the Laboratoire de Mecanique et d'Acoustique [1]. The aim was to achieve a silent zone using seven error microphones and six secondary loudspeakers, the primary noise coming from one or two loudspeakers. We expected from these experiments to show the spatial extent of the control, the limit with the frequency, and the ability of different algorithms to deal with the noise coming from two uncorrelated noise sources.
Achieving a silent zone in free-field is a contemporary topic in the field of active noise control as showing the numerous articles dealing with control barriers, see for example [2].
The aim of my study at the ISVR was to develop a programme to predict the soundfield when active control is performed in free field.

1 Single channel case

In this section, we consider the case of a single channel system illustrated in figure 1: one microphone and one secondary source are used to minimize the noise coming from a primary source.

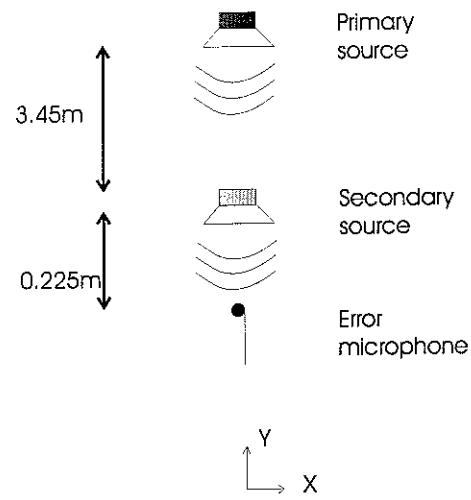

Figure 1:

The calculation of the value q_{s0} of the secondary source strength q_s that cancels the pressure due to the primary source at the error microphone position is straight forward.

$$p_{err} = Z_p\, q_p + Z_s\, q_s$$

where p_{err} denotes the pressure at the error microphone, q_p and q_s the primary and the secondary source strengths, Z_p and Z_s the primary and secondary complex transfer acoustic impedance. To obtain $p_{err} = 0$, we must have

$$q_{s0} = -Z_s^{-1}\, Z_p\, q_p$$

We are interested in the effect of frequency on the size of the quiet zone area. Figure 2 plots the attenuation $att = 20\ log_{10} \left| \frac{p_{on}}{p_{off}} \right|$ where p_{on} is the pressure with control and p_{off} is the pressure without control.

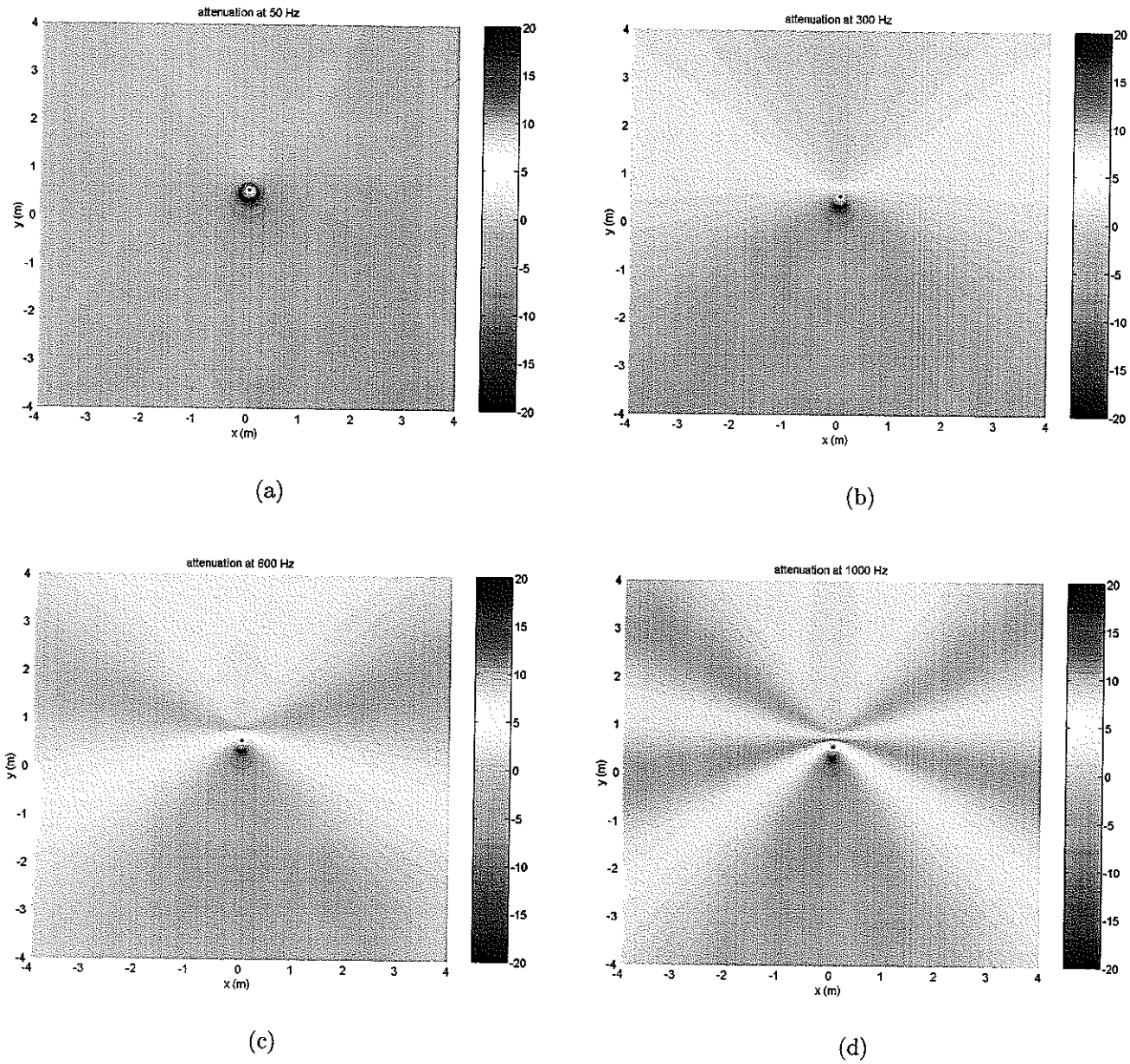

Figure 2: Size of the quiet zone area at 50 Hz (a), 300 Hz (b), 600 Hz (c) and 1000 Hz (d)

Figure 2 shows the results of a series of simulations. The conclusion is as expected: the higher is the frequency, the smaller is the quiet zone area.

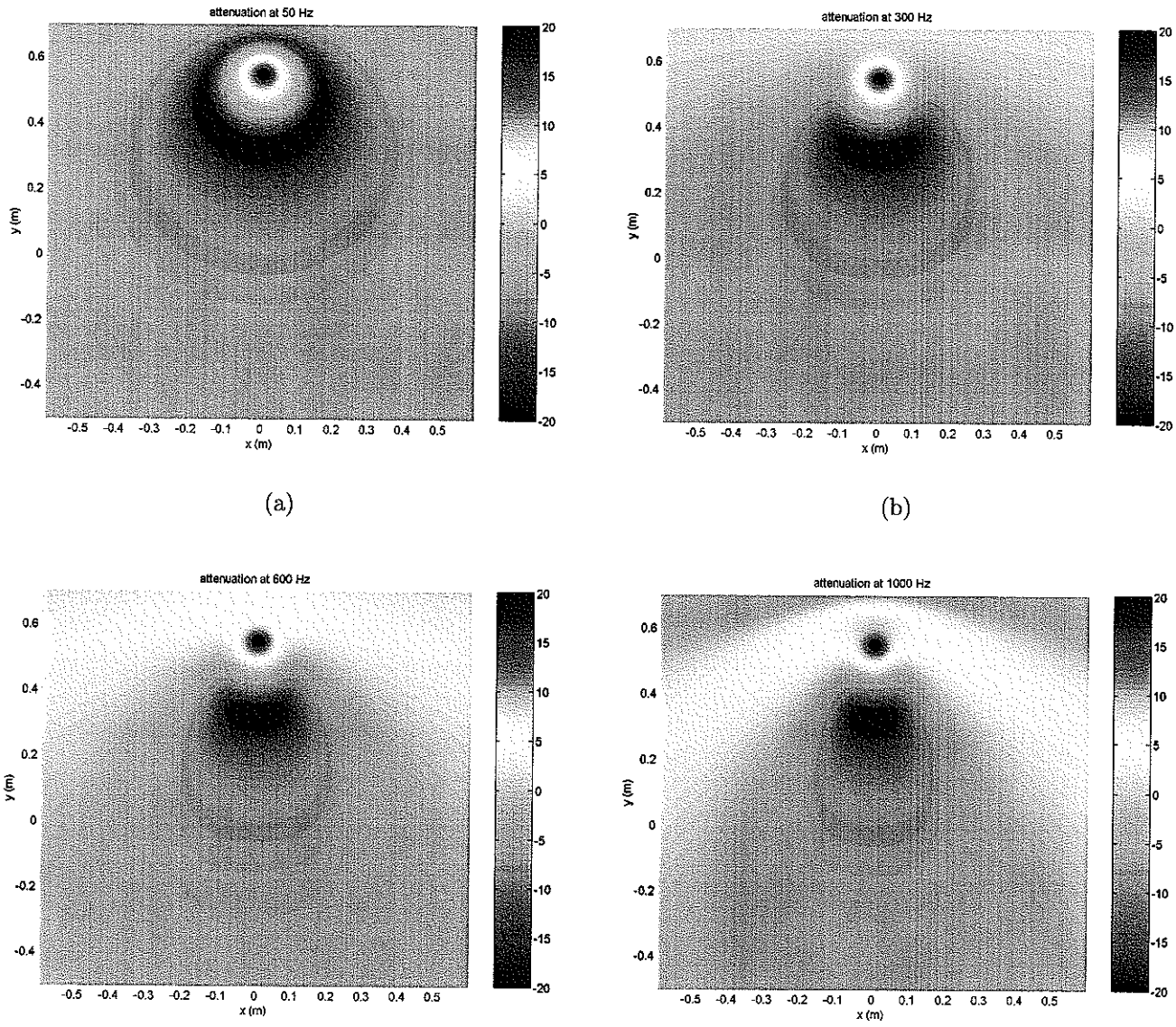

(a) (b) (c) (d)

Figure 3: quiet zone in near field at 50 Hz (a), 300 Hz (b), 600 Hz (c) and 1000 Hz (d)

At high frequencies, we can see interferences between the primary and the secondary sources. In the y direction, which is the axis of the two sources, we can see on figure 3 that the peaks of the waves are separated from approximately half a wavelength $\lambda/2$ since wave from secondary source travels in opposite direction to primary wave. In the x direction, the peaks of the waves are separated from approximately a wavelength λ because primary wave has equal phase interferences with secondary wave.

2 Multi-channel case : under-determined system

In this section, we consider the case of an under-determined multi-channel system illustrated in figure 4: one microphone and two secondary sources are used to minimize the noise coming from a primary source.

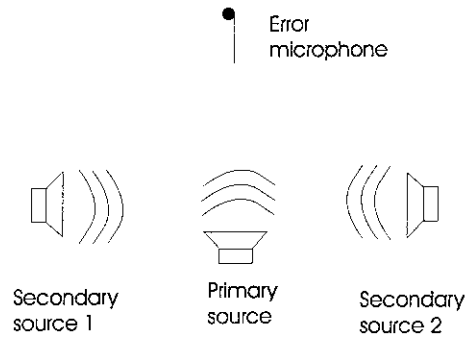

Figure 4:

This time, the error pressure is:

$$p_{err} = Z_p\, q_p + Z_{s1}\, q_{s1} + Z_{s2}\, q_{s2}$$

We now want to determinate the vector (q_{s0_1}, q_{s0_2}) that minimizes the error pressure. The system is clearly under-determined: there are more unknowns than equations. For symmetric reasons we can assume $q_{s1} = q_{s2}$. With this assumption, we obtain the results shown in the figure 5 which illustrates the decreasing of the control effect with the frequency.

3 Multi-channel case : over-determined system

For the simulations of the over-determined system, we consider the case of an over-determined multi-channel system illustrated in figure 6 : twenty microphones and two secondary sources are used to minimize the noise coming from a primary source.
The twenty microphones are situated on a 2D-circle in the far-field of the primary source ; at the center of the circle is the primary source with the two secondary sources around it.
The total attenuation on the error microphones is defined as :

$$att_{min} = \frac{\sum_{i=1}^{20} |p_{on_i}|^2}{\sum_{i=1}^{20} |p_{off_i}|^2}$$

where p_{on_i} is the pressure after control on the error microphone i and p_{off_i} is the pressure before control on the error microphone i.
The figure 7 plots the total attenuation with kd (plain line) and the theoretical minimum power output (dashed line). According to [3], the theoretical minimum power output can be expressed relative to the power output produced by the primary source and is given by

$$\frac{W_0}{W_{PP\,theory}} = 1 - \left(\frac{2sinc^2(kd)}{1 + sinc(2kd)} \right)$$

We can see in figure 7 that the shapes of the curves are similar. However, the values of kd of

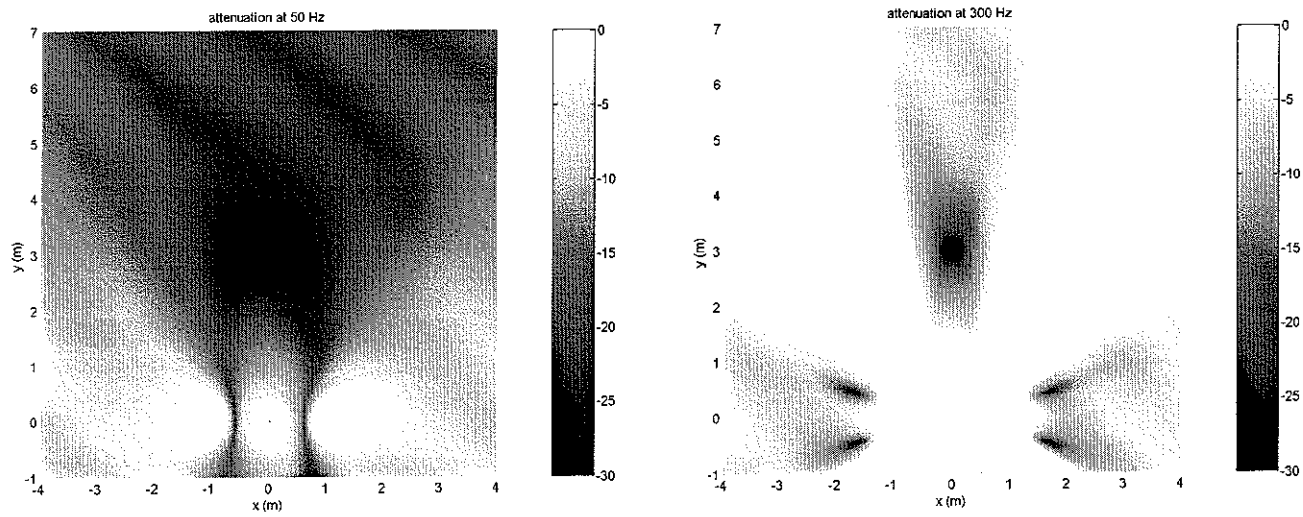

(a) (b)

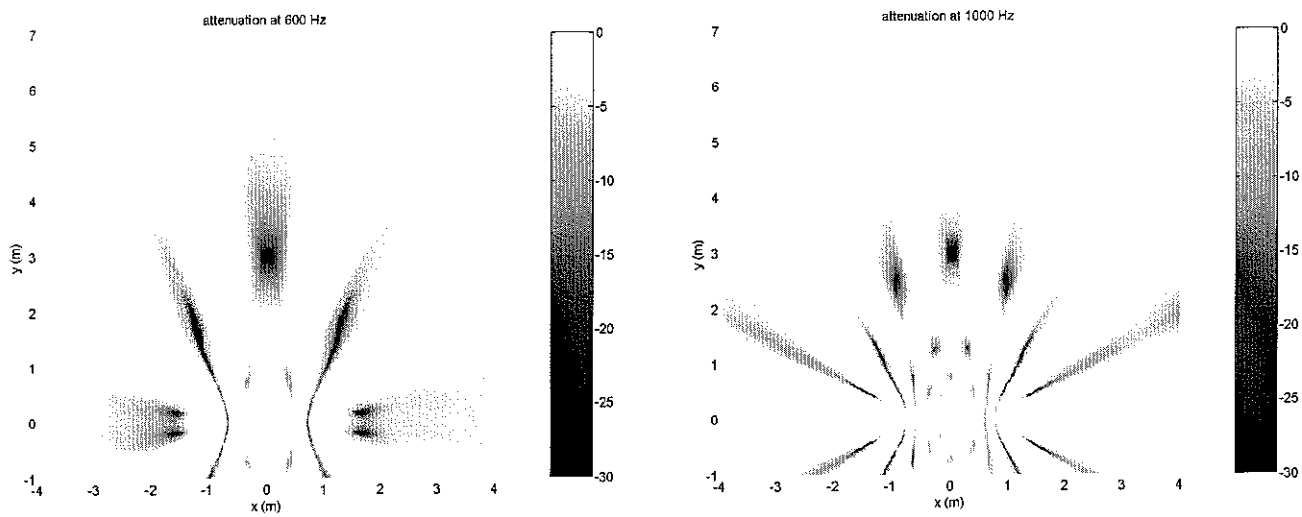

(c) (d)

Figure 5: Attenuation at 50 Hz (a), 300 Hz (b), 600 Hz (c) and 1000 Hz (d)

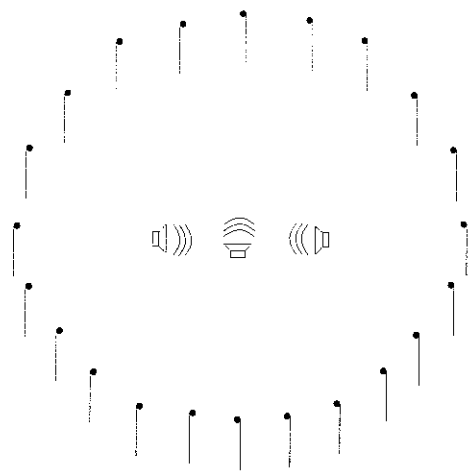

Figure 6:

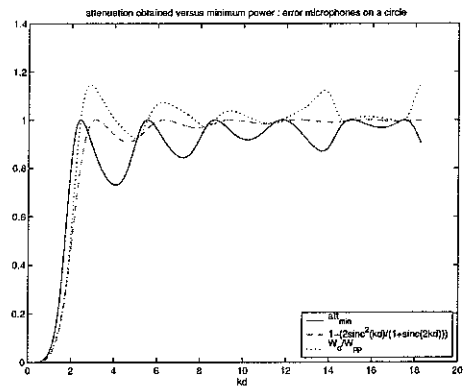

Figure 7: total attenuation and minimum power output

maximum attenuation are not exactly the same than the values of kd of minimum power. We can also calculate the minimum power output but this time using the secondary strengths obtained for the corresponding maximum attenuation. This is the dotted line in figure 7.
We can conclude that the maximum attenuation at the error microphones is not obtained with the minimum power output. There must be areas where the level of sound is increased.

We have done the same simulations, but this time, 10 error microphones were located on a half sphere in the far-field of the primary source. The microphones are equally distributed on the hemisphere, their positions given by [4].

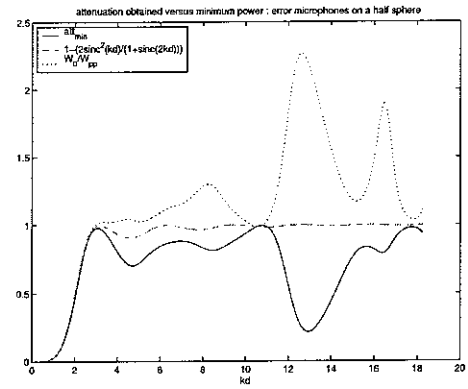

Figure 8: total attenuation and minimum power output

The figure 8 shows that the total attenuation and the minimum power output fits perfectly for low values of kd. Relative maxima of the total attenuation are obtained for the same values of kd than those corresponding to minimum power output. It is not true for high values of kd. Plotting again the minimum power output using the secondary strengths obtained for the corresponding maximum attenuation (dotted line), we arrive to the same conclusion : the maximum attenuation at the error microphones is not obtained with the minimum power output. There must be areas where the level of sound is increased.
The same simulations with 19 microphones located on a whole sphere give the same results, as shown in figure 9.

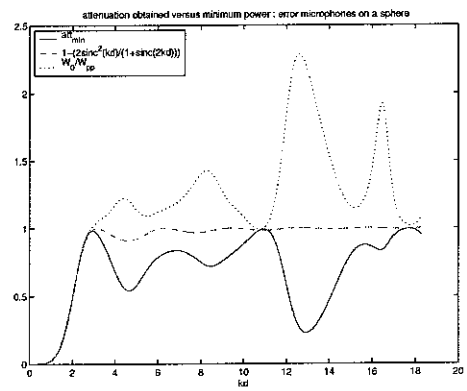

Figure 9: total attenuation and minimum power output

4 Multi-channel case : simulations with experimental design

In this section, we chose the experimental design we have tested in an anechoic theatre, as shown in figure 10.

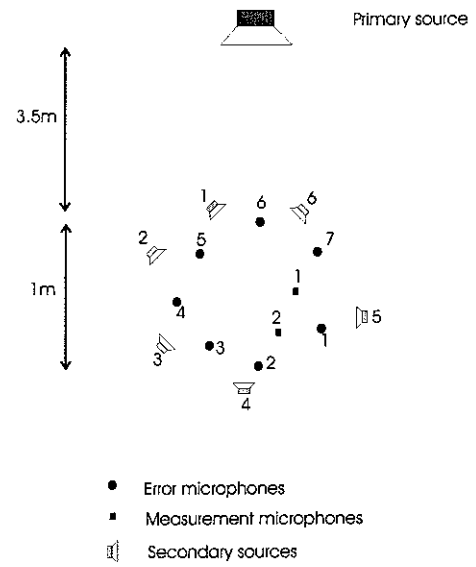

Figure 10: experimental design

The aim of the experiment was to create a silent zone in an anechoic room in presence of random noise coming from one or two decorrelated sources. The sum of squared pressures at 7 error microphones was minimized by 6 secondary sources, and the effect was measured at 2 measurement microphones.

4.1 Results of simulations

Figure 11 shows the decreasing of the quiet zone areas with the frequency. The places where the secondary sources are located appear clearly.
Figure 12 shows the same simulations in near field. The exact positions of error microphones are represented by crosses and the positions of the measurement microphones are represented by stars. We can see how the control manage to create a quiet zone covering all at low frequencies and then how it becomes local. At 600 Hz, the control is no more efficient for the measurement microphone 2.
Next simulations are simulations of the control for frequencies from 0 to 1000 Hz.

The plain line in figure 13 is the attenuation for each error microphone as a function of the excitation frequency, obtained during experiments.
The dashed line in figure 13 is the attenuation for each error microphone as a function of the excitation frequency, obtained according to numerical simulation.

The figure 14 shows the attenuation of the sum squared error signals. Plain line refers to experiments and dashed line to simulations.
The plain line in figure 15 is the attenuation for each measurement microphone as a function of the excitation frequency, obtained during experiments.

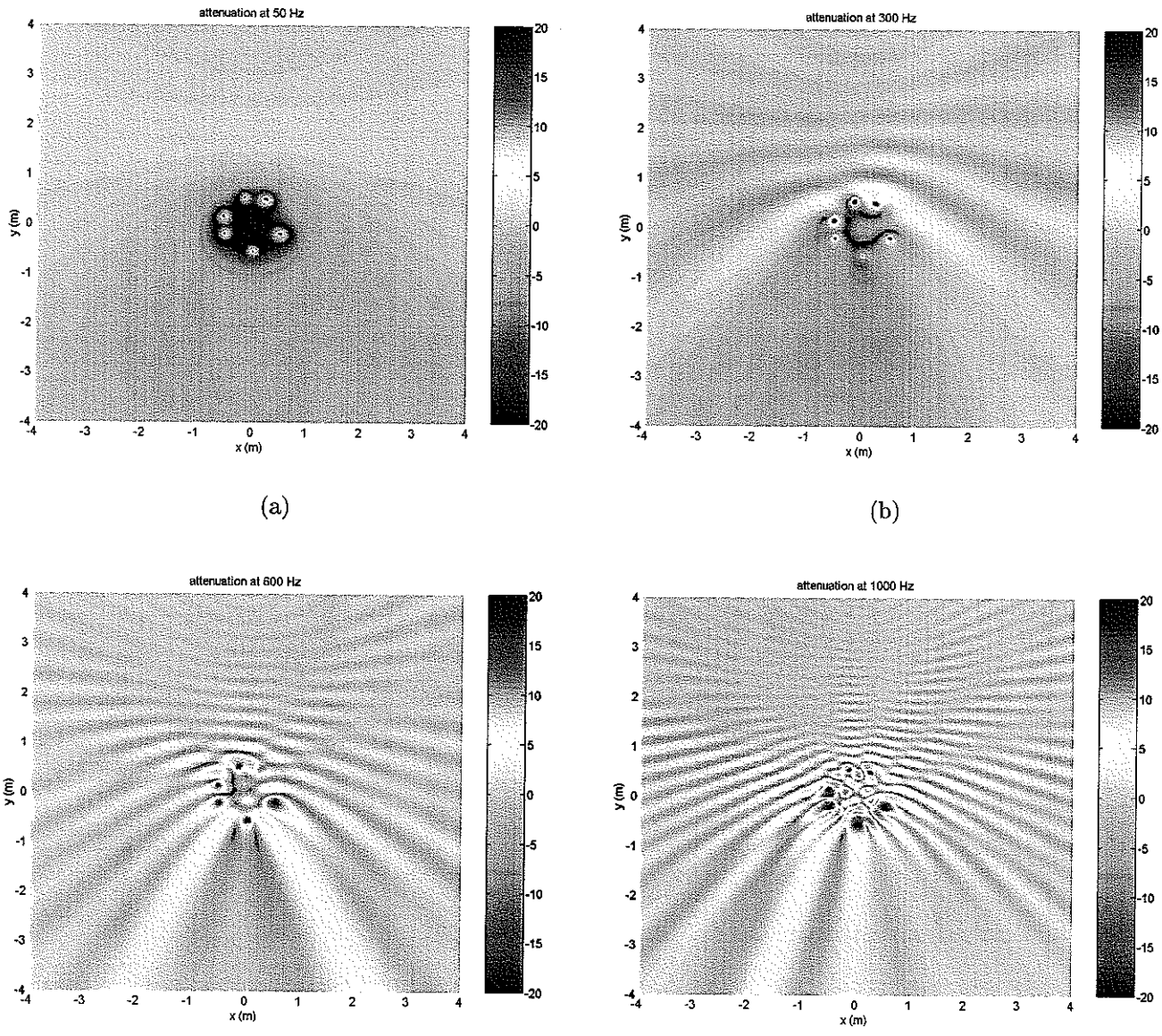

Figure 11: Size of the quiet zone at 50 Hz (a), 300 Hz (b), 600 Hz (c) and 1000 Hz (d)

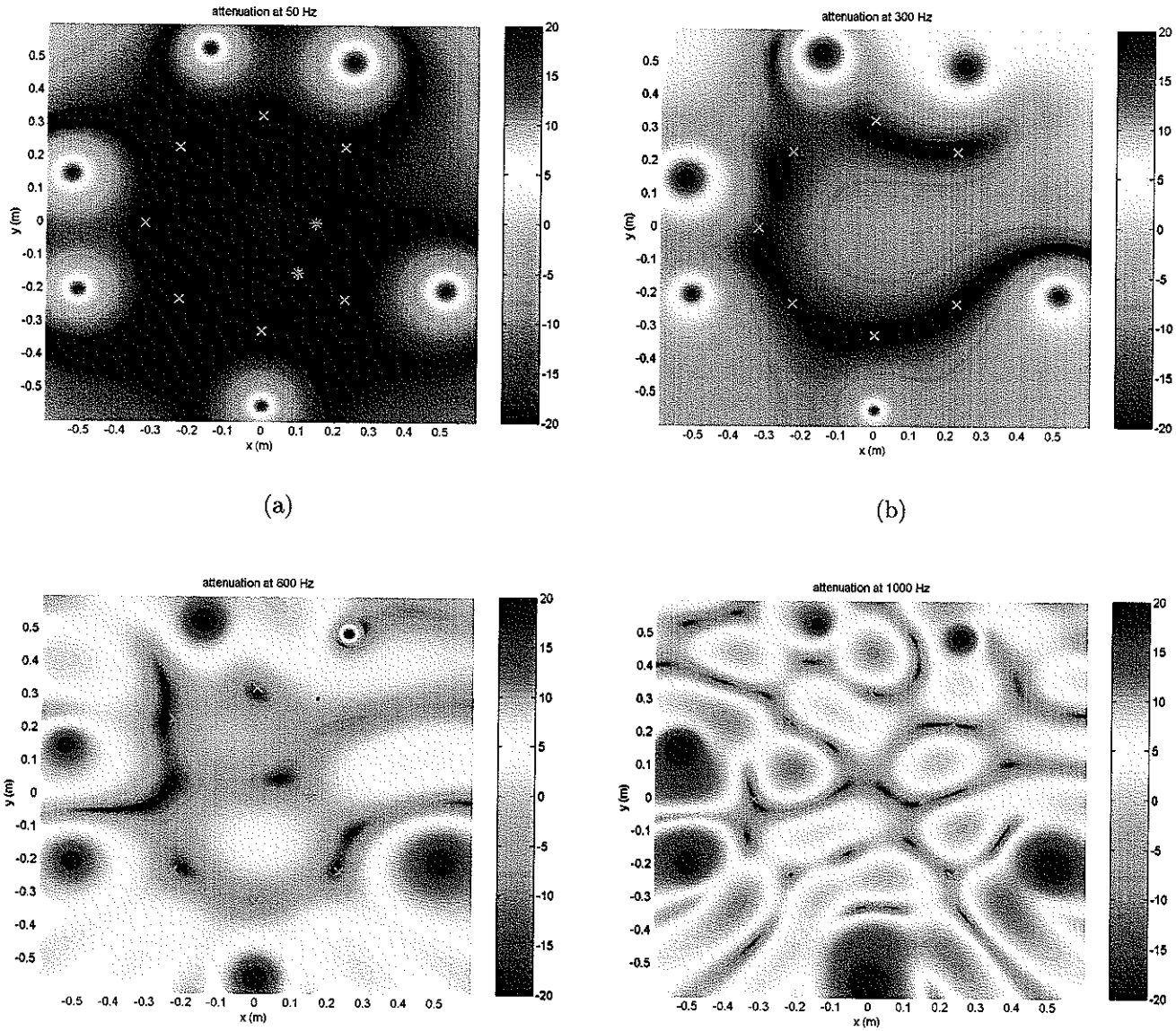

(a) (b)

(c) (d)

Figure 12: Zoom-in of the quiet zone at 50 Hz (a), 300 Hz (b), 600 Hz (c) and 1000 Hz (d)

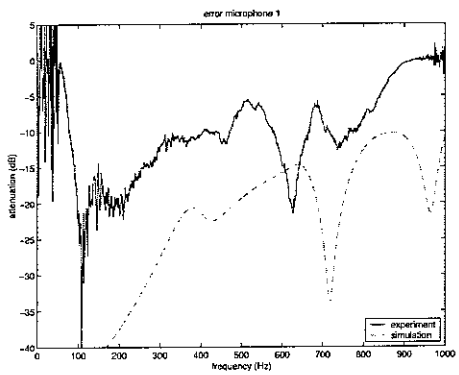

(a)

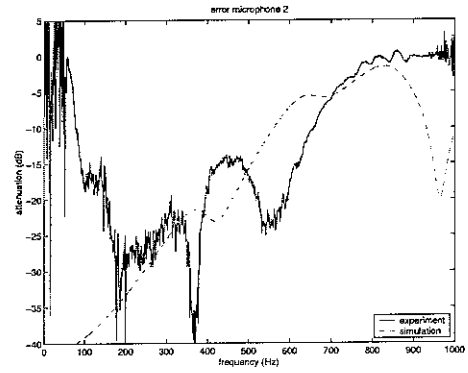

(b)

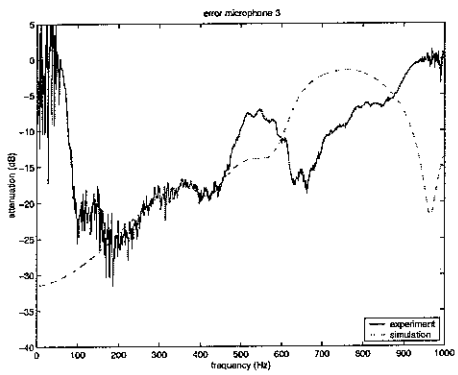

(c)

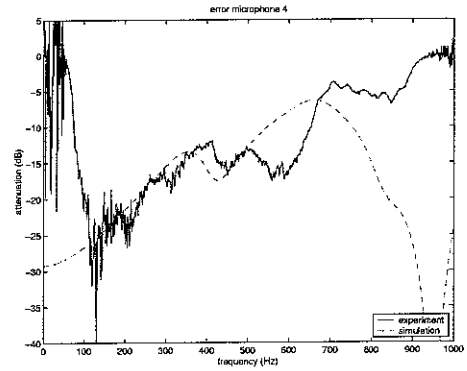

(d)

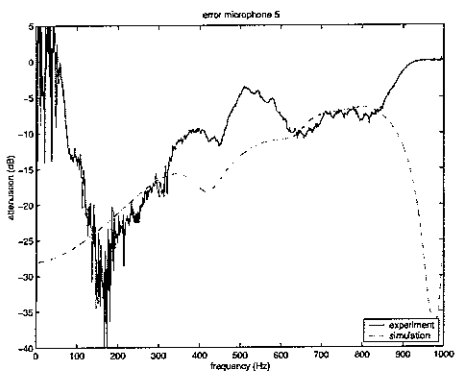

(e)

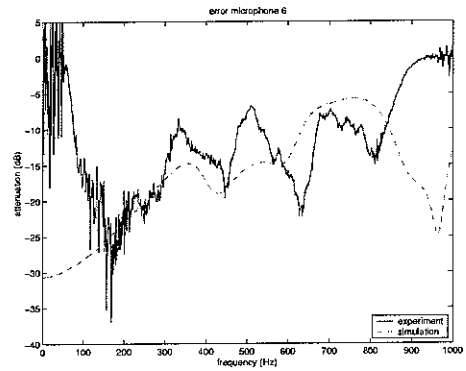

(f)

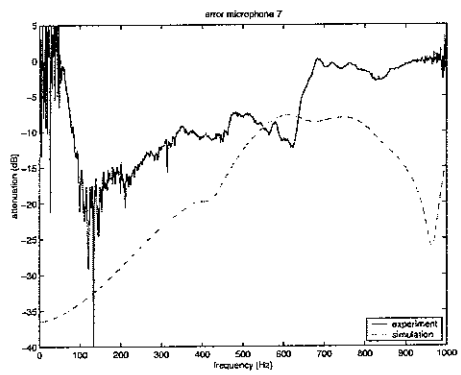

(g)

Figure 13: Attenuation at each error microphone

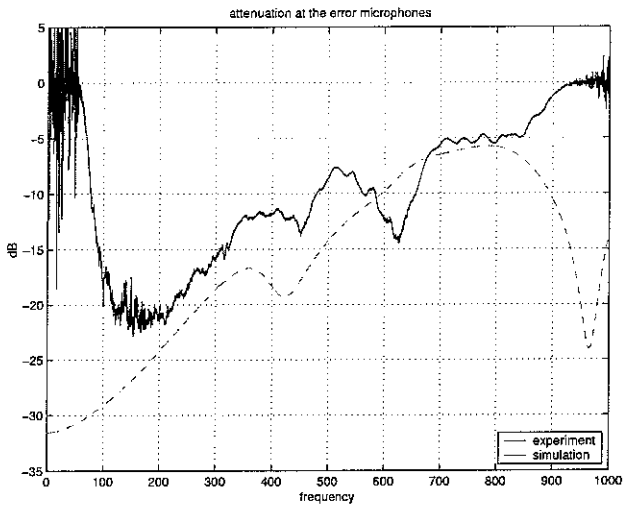

Figure 14: Attenuation at the error microphones

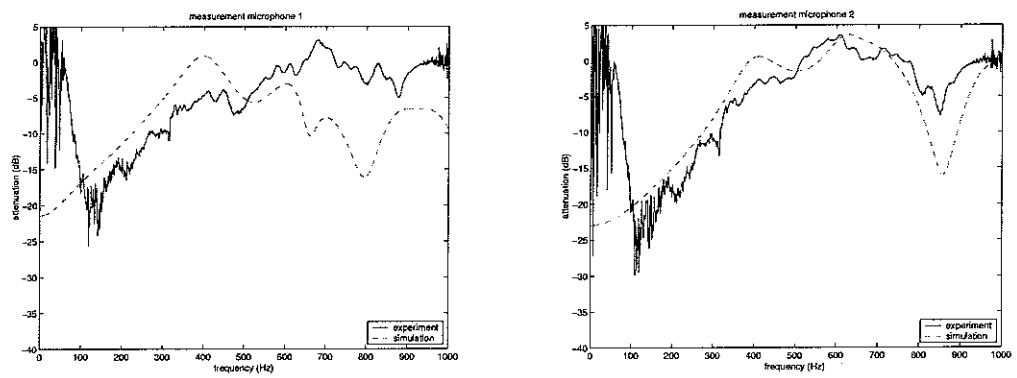

(a) (b)

Figure 15: Attenuation at measurement microphones

The dashed line in figure 15 is the attenuation for each measurement microphone as a function of the excitation frequency, obtained according to numerical simulation.
There are several explanations to the differences between the simulation and the experimental plots. In experiments, at low frequency (below 80 Hz), there are no attenuation because the controller is clearly inefficient in this frequency domain. The big gap between the two lines in figure 13 for error microphone 1 is perhaps due to a microphone position which is not exactly that we have measured. The effect of the ground is not taken into account in simulations. There could have been also unwanted noise in the anechoic room.

5 Optimal controller

5.1 One primary source and one reference microphone

In this section, we calculate the optimal controller W_{opt} when the reference signal is not taken directly from the primary source but from a reference microphone.
According to [5],

$$W_{opt} = -\left[G^H G\right]^{-1} G^H S_{xd} S_{xx}^{-1}$$

where G is the matrix of frequency response functions of the plant, S_{xx} is the matrix of cross spectral densities for the reference signals x and S_{xd} is the matrix of cross spectral densities between the disturbance d and reference signals.

The effect of the control at the error microphones can be then calculated by :

$$p_{err}^{on} = p_{err}^{off} + G W_{opt} Z_{pri-err}$$

where $Z_{pri-err}$ is the transfer impedance between the primary source and the error microphone.

As far as there is no causality constraint, using a reference microphone is leading to the maximal attenuation we can obtain (shown in figure 16) wherever this reference microphone is located.

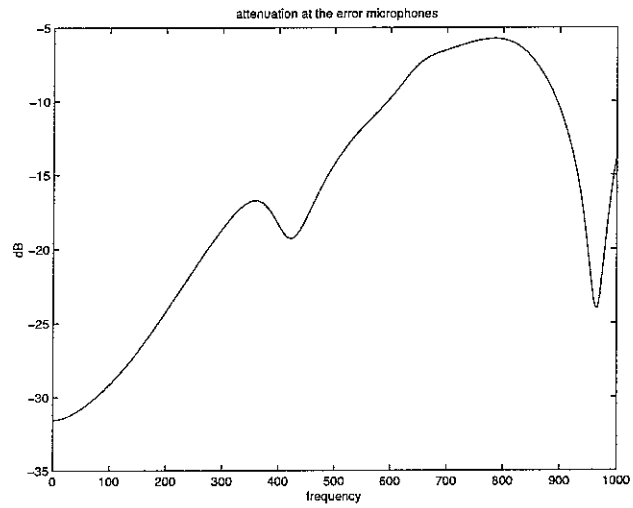

Figure 16: Attenuation at the error microphones

5.2 Two primary sources and one reference microphone

Adding another primary source leads to less attenuation at the error microphone, especially when a source is very close to the reference microphone compared to the other.
The figure 17 shows the attenuation at the error microphones obtained when there is (a) one primary source, (b) one source very close to the reference microphone (10 cm) while the other is located at 2m from the reference microphone and (c) two sources are at equal distance from the reference microphone.

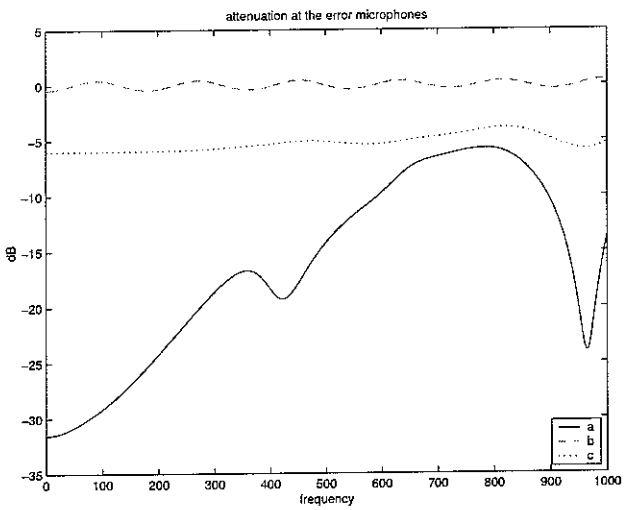

Figure 17: Attenuation at the error microphones

6 Conclusion

We have developed a model that allow to predict results from active control experiments in free field. These results are in good agreement with the experimental results obtained. This is a capital result because we can conclude that during experiments, the limiting factor was acoustic rather than technology.

References

[1] E.Friot, C.Bordier, "CONFINING SILENCE": A FREE-FIELD EXPERIMENT OF MULTICHANNEL CONTROL FOR RANDOM NOISE COMING FROM UNCORRELATED SOURCES IN AN ANECHOIC THEATRE, *Proceedings of ACTIVE2002*, 2002

[2] S. E. Wright, ACTIVE CONTROL OF ENVIRONMENTAL NOISE, VI: PERFORMANCE OF A FUNDAMENTAL FREE-FIELD SOUND CANCELLING SYSTEM, *Journal of Sound and Vibration*, Vol. 245, No. 4, pp. 581-609, 2001

[3] P. A. Nelson & S. J. Elliott, ACTIVE CONTROL OF SOUND, Academic Press, 1992

[4] J. R. Hassal & K. Zaveri, ACOUSTIC NOISE MEASUREMENT, Bruel & Kjaer, 1979

[5] S. J. Elliott, SIGNAL PROCESSING FOR ACTIVE CONTROL, Academic Press, 2001